Coulomb blockade related to mutual Coulomb interaction in an external environment in an array of single tunnel junctions connected to Ni nanowires

Junji Haruyama, Ken-ichiro Hijioka, Motohiro Tako, and Yuki Sato
Department of Electrical Engineering and Electronics, Aoyama Gakuin University, 6-16-1 Chitosedai, Setagaya, Tokyo 157-8572 Japan
(Received 24 March 1999; revised manuscript received 28 July 1999)

The Coulomb blockade (CB), which depends on the mutual Coulomb interaction (MCI) in external electromagnetic environments (EME's), is reported in an array system of single tunnel junctions connected directly to disordered Ni nanowires (i.e., an array of a disordered Ni nanowire/Al_2O_3/Al system located in parallel), fabricated using a nanoporous Al film template. The observed zero-bias conductance (G_0) anomaly and its linear G_0 versus temperature relation qualitatively agree with the CB observations of Zeller and Giaever and of Cleland, Schmidt, and Clarke. The CB is also quantitatively confirmed from the extended Zeller-Giaever model in a tunnel-junction array. In the high-voltage region, only one-dimensional (1D) MCI following the Altshuler-Aronov formula in a disordered Ni wire dominates the conductance mechanism with the absence of the CB. In contrast, in the lower-voltage region, the CB mentioned above emerges at temperatures below a phase-transition temperature (T_c), accompanied by the 1D MCI in the Ni wire. The MCI plays the key roles of high-impedance EME and transmission line following the phase correlation theory of the CB. It is found that the CB is very sensitive to the diffusion coefficient (D) of the MCI, resulting in the linear T_c-vs-$D^{1/2}$ relation. For this relation, we propose as one possible model, that the charging energy of the CB competes with the energy quantum of fluctuation of the Nyquist phase breaking caused by multiple Coulomb scattering in the Ni nanowire. This linear T_c-vs-$D^{1/2}$ relation is reconfirmed by the Ni-wire diameter dependence of T_c. The magnetic field dependence of the G_0-versus-temperature relation obviously supports the actual presence of T_c with different conductance mechanisms for the temperatures above and below T_c.

I. INTRODUCTION

The Coulomb blockade (CB) has been experimentally reported in a variety of nanotunnel junction systems (e.g., metal nanoparticle array systems, quantum dots, and the other nanojunction systems fabricated by semiconductor nanotechnologies and scanning probe microscopes). It is also successfully understood by many theoretical works (e.g., the orthodox theory proposed by Averin and Likharev).[1] Most experiments have been basically performed in multitunnel junction (MTJ) systems. For instance, Zeller and Giaever first reported a zero-bias conductance (G_0) anomaly and its linear G_0 versus temperature relation in the array of Sn nanopartcles located in parallel.[15] They explained the G_0 anomaly by introducing the charging effect of the nanoparticle (i.e., capacitance model). The linear G_0-versus-temperature relation was also interpreted by the contribution of many nanoparticles with distributed charging energy (E_C). In contrast, only a few have been reports successfully given on the CB in a single tunnel junction (STJ) system, because it is difficult to fabricate an external electromagnetic environment (EME) satisfying the phase correlation (PC) theory of the CB in a single-junction system. In PC theory, unless the real part of the total impedance of the EME ($\mathrm{Re}[Z_t(\omega)]$) is larger than the resistance quantum $R_Q \sim h/e^2 = 25.8\,\mathrm{k}\Omega$, the tunneling electron cannot transfer its energy to the external environment (EME). In addition, unless the high-impedance transmission line ($R_L > R_Q$) is closely connected to a single junction, zero-point oscillations caused by the EME fluctuation modify the surface charges on the junction. They easily smear out the CB.[2,3] Furthermore, the geometry of the high $\mathrm{Re}[Z_t(\omega)]$ including the high-R_L region also must have enough small parasitic capacitance to observe a clear CB.[18] Cleland, Schmidt, and Clarke successfully reported on the G_0 anomaly and CB in one single-junction system, developing the PC theory.[3] The first goal of this work is to report on the G_0 anomaly and its linear G_0-versus-temperature relation in an array of single junctions located in parallel, which was never fabricated in past work, and to identify it as the CB. These findings are actually consistent with the reports by Zeller and Giaever and by Cleland, Schmidt, and Clarke in some respect, suggesting the presence of a CB.

Here, since the CB is very sensitive to the external environment (EME) as mentioned above, correlation of CB with the mesoscopic phenomena in the EME has recently attracted much attention.[4–9] In multijunction systems, some works successfully revealed the correlation of the CB with the phase interference of electron waves,[4] the spin interaction of electrons,[6] and the fluctuation (e.g., electron phase coherence, which is never destroyed even in a quantum dot inserted in an Aharanov-Bohm ring except for the case of spin coherence,[4] and the many-body effect in an artificial atom[6]). On the other hand, in the single-junction system, our past work has experimentally reported on the CB associated with the repulsive mutual Coulomb interaction (MCI) in the EME and with the extended PC theory proposed by Nazarov.[10–12] The second goal of this work is to clarify the detailed correlation of the CB with the MCI in an external environment, based on the confirmation of the CB mentioned above.

In our previous works, we briefly discussed the CB and its correlation with the MCI in the same system as that in this work (i.e., an array of Al/Al_2O_3/Ni nanowire STJs),[10–12]

from the following two viewpoints.

(1) *Nazarov's theory*.[11,13] In PC theory, the external environment (EME) plays two key roles for the CB in a STJ: (a) the tunneling electron transfers its energy to the EME, leading to the CB, and (b) EME phase fluctuations ($\tilde{\varphi}$) causes a charge fluctuation ($\tilde{Q}$) on the junction surface by coupling with zero-point oscillation (or by the commutation relation $[\tilde{\varphi},\tilde{Q}]=ie$), smearing out the CB. For the first process, $\mathrm{Re}[Z_t(\omega)]$ must be larger than R_Q and to avoid the second process, high R_L must be closely connected to a single junction. Since this connection of high R_L automatically results in high $\mathrm{Re}[Z_t(\omega)]$, the first process can also occur for high R_L. Nazarov extended this PC theory to the CB, which depends on the MCI in the external environment.[13] We fitted the second derivative of measured current (d^2I/dV^2) in our samples with different wire diameters by his theory at a fixed temperature ($T=1.5$ K) and identified the tunnel structure parameters.[11] Since they were in good agreement and reasonable values, we concluded that the results concur with a CB related to the MCI following Nazarov's theory.

(2) Comparison with previous reports of the CB and the theory for MCI in disordered conductors.[10,14] The linear G_0-versus-temperature relation observed was very roughly compared with two previous experimental results[3,15] and identified as a CB.[10] The presence of MCI in the Ni nanowire was also identified from the G-vs-$V^{1/2}$ curve fitting by the Altshuler-Aronov theory. We pointed out a possibility that the MCI plays the role of high R_L for the CB. The Altshuler-Aronov theory basically employs a calculation of the density of states in which MCI was treated as its quantum correction.[14] Hence, it is very different from Nazarov's theory, because the charging effect E_C of the tunnel junction capacitance was never considered. In this viewpoint, the CB and MCI were separately discussed. Also, other necessary conditions for a CB were discussed (e.g., the influence of many STJ's located in parallel and the parasitic capacitance of the long resistive Ni wire on the CB).[10]

Although they discussed the presence of the CB related to the MCI, no detailed features of the CB, MCI, and their correlation were clarified. In particular, the correlation of the temperature dependence was never reported. In this work, we clarify these points focusing on the temperature dependence of resistance (conductance), taking into account the Altshuler and CB theories. In Sec. II, experimental results are presented. In Sec. III A, G_0 anomaly and the linear G_0-versus temperature relation are discussed based on the CB observations of Zeller and Giaever and of Cleland, Schmidt, and Clarke. Based on the extended Zeller-Giaever capacitance model, it is quantitatively confirmed that the G_0 anomaly originated from the CB in the array of junctions located in parallel with distributed E_C. The high-resistance Ni wire ($>R_Q$) plays the role of the high $\mathrm{Re}[Z_t(\omega)]$ and R_L for the CB. In Sec. II B, the one-dimensional (1D) MCI following Altshuler's theory is discussed, based on the temperature dependence of the normalized resistance in the high-voltage region. In contrast, in Sec. II C, the case at low voltages is discussed. The appearance of the CB at the temperatures below a phase-transition temperature (T_c) is identified with the 1D MCI at high temperatures ($>T_c$). The MCI is the origin of the high resistance of the Ni wire. In Sec. III D, correlation of the CB with the 1D MCI is discussed. The CB is sensitive to a diffusion coefficient (D) of the MCI, resulting in the linear T_c-vs-$D^{1/2}$ relation. The origin of linear T_c-vs-$D^{1/2}$ relation is interpreted as coming from the comparison of E_c with an energy quantum of phase fluctuation caused by the MCI. In Sec. III E, the linear T_c-vs-$D^{1/2}$ relation is reconfirmed by the linear wire diameter dependence of T_c. In Sec. III F, the presence of T_c and different conductance mechanisms classified at T_c are obviously reconfirmed by the magnetic field dependence of the G_0-versus-temperature relation.

II. EXPERIMENTAL RESULTS

A. Sample structure and measurement method

Figure 1(a) shows a schematic overview of the sample structure fabricated by using a nanomaterial [i.e., a nanoporous alumina film template (NAT)].[10–12] The NAT with high packing density of nanosized diameter pores was simply fabricated by anodizing a pure Al substrate in H_2SO_4. Each pore automatically has a single tunnel barrier layer between its bottom and the Al substrate. Because of the self-organized growth, this NAT exhibits high uniformity, high repeatability, and high controllability of the nanostructure parameters (e.g., pore diameter and thickness of the tunnel barrier layer). In this work, Ni was electrochemically deposited into the nanopores. Thus, this system is an array of Ni nanowire/Al_2O_3/Al structure (single junctions connected directly to Ni nanowires) located in parallel. The structure parameters of the Ni wire and the tunnel junction were confirmed by atomic force microscopy (AFM), scanning electron microscopy (SEM), and high-resolution cross-sectional transmission electron microscopy (TEM).[10–12]

Figure 1(b) shows a typical high-resolution cross-sectional TEM image of one Ni wire including the bottom part. One can actually observe the tunnel barrier layer and Ni nanowire of the order of 10 nm in the thickness and the diameter, respectively. In addition, very small interference patterns on the order of subnanometer diameter are visible in the Ni wire. It suggests that the Ni wire is in a disordered structure. This, however, never points to the presence of electrical discontinuity grains, because the thickness of a grain boundary is thin, in the subnanometer range, and any insulator layers cannot be introduced in our electrochemical deposition process. It also never indicates subnanoparticle arrays with a charging effect like the Zeller-Giaever system, because such thin boundary layers in Ni cannot quantitatively have a tunnel resistance larger than R_Q. Furthermore, no Coulomb staircase (conductance oscillation) is observable in any current-versus-voltage (conductance-versus-voltage) curves unlike the many previous reports of a metal nanoparticle array,[10] as mentioned in the next section. These findings strongly support that the Ni wire is electrically continuous in spite of a disordered structure, and our system is then purely a single junction/Ni nanowire array system. It is the foundation for our argument.

All electrical measurements were carried out by applying a dc voltage between the Al substrate and the top of all Ni wires, as shown in Fig. 1(a). The number of electrically active wire and junction systems is estimated from the ob-

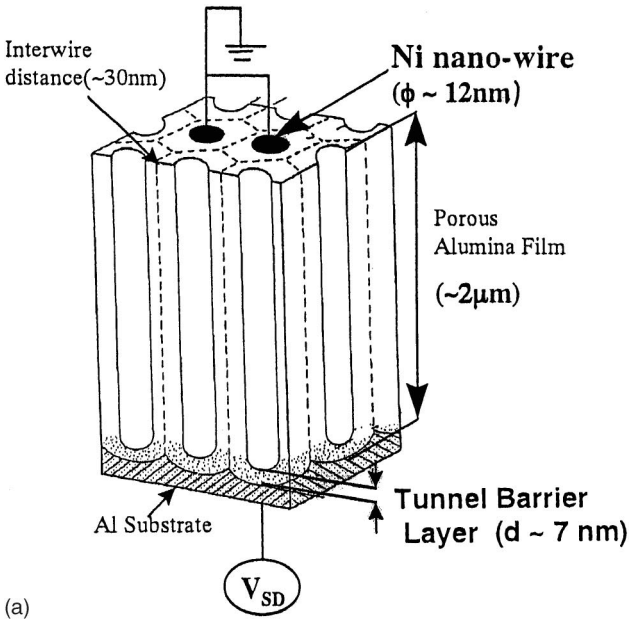

(a)

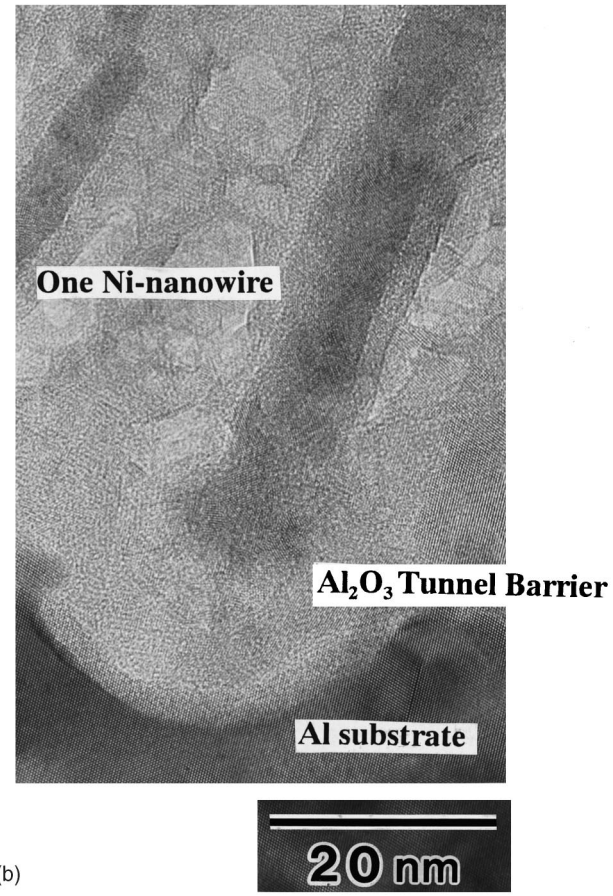

(b)

FIG. 1. (a) Schematic overview of a sample structure, an array system of Ni-nanowire/Al_2O_3/Al (single tunnel junctions directly connected to Ni nanowires) located in parallel. It was fabricated using a nanoporous alumina film template, which simply provides unique nanostructures by self-organized growth. (b) High-resolution cross-sectional TEM image of one Ni nanowire, including the tunnel barrier layer at the bottom. One can actually see a tunnel barrier and nanowire on the order of 10 nm.

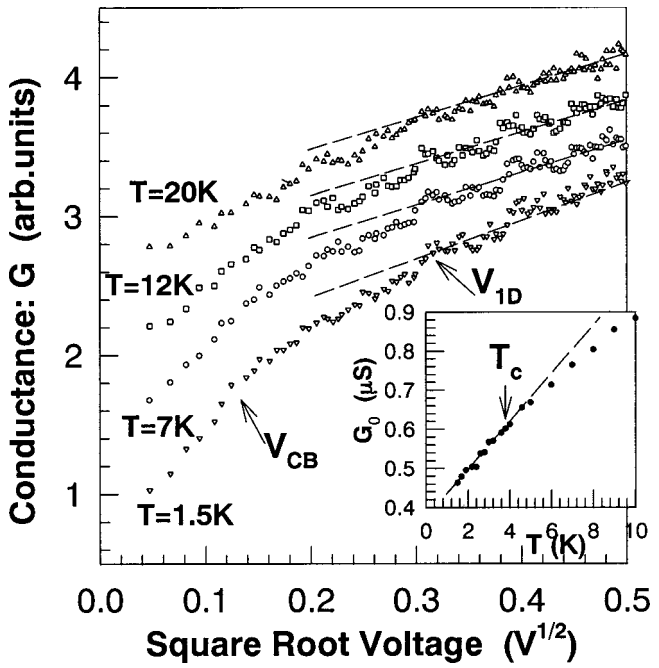

FIG. 2. Temperature dependence of conductance (G) vs $V^{1/2}$ features in the positive-voltage region, exhibiting the G_0 anomaly. The corner voltages (V_{CB} and V_{1D}) were interpreted as the transition voltages from the 1D MCI to the CB regimes and from the 3D to the 1D MCI regimes, respectively. Inset: Temperature dependence of G_0. The linear G_0-vs-temperature relation as shown by the dotted line is interpreted as evidence for the CB in the tunnel-junction array.

served current order to be at most on the order of 10^4. The magnetic field (B) was applied perpendicularly to the axis of the Ni wire.

B. Measurement results and analyses

Figure 2 shows the temperature (T) dependence of conductance (G)-versus-$V^{1/2}$ curve in the positive-voltage region. They obviously exhibit the G_0 anomalies. One corner voltage noted as V_{1D} is observed around 0.3 V at each temperature, whereas the other corner voltage noted as V_{CB} emerges around 0.12 V only at $T=1.5$ K. No conductance oscillation is observable in any curves as mentioned in Sec. II A. Although small conductance oscillations are observed at some voltage points, they originate from the simple measurement noise because they are independent of temperature. The inset of Fig. 2 shows the temperature (T) dependence of G_0. The relation is mostly linear at the temperatures below about 4 K, because this low-temperature region could not be fitted by any functions related to the CB, electron transport in disordered conductors, and hopping conductance [e.g., G vs $T^{1/2}$, G vs $T^{1/4}$, G vs ln(T), R vs $T^{-1/4}$ (Refs. 1, 14, and 16)] and only the linear relation gave the best fit. The interpretation of this linear G_0-vs-T relation as the CB is discussed in Sec. III A.

Figure 3 shows the temperature dependence of the normalized resistance at each voltage point, which is below and slightly above V_{CB}, in Fig. 2. Data fitting by Eq. (1), which is Altshuler's formula for the 1D MCI in disordered conductors, basically gave the best fit to the linear $\delta R/R_n$-vs-$T^{1/2}$ parts:

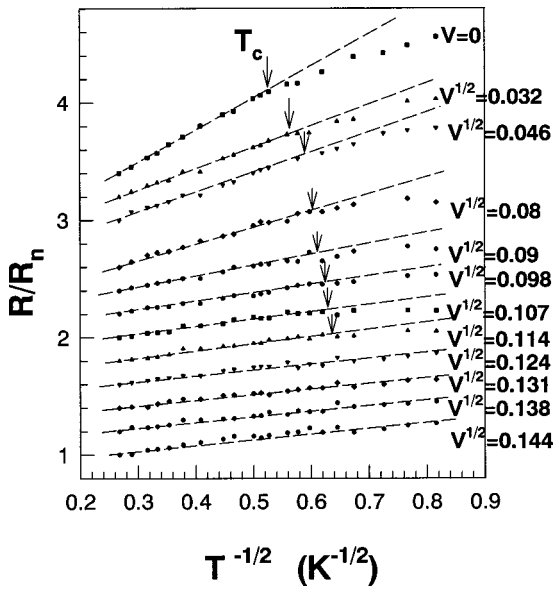

FIG. 3. Temperature dependence of the normalized resistance at each voltage in Fig. 2. The lower four and upper eight features were measured at the voltage points above and below V_{CB}, respectively. The dotted line shows the best fitting by the Altshuler-Aronov formula for the 1D MCI in disordered conductors. The arrows indicate phase-transition temperatures (T_c) from the 1D MCI to the CB temperature regimes.

$$\delta R(T)/R_n=(\rho e^2/8\hbar A)(4+3\lambda/2)(D\hbar/T)^{1/2}, \qquad (1)$$

where R_n, ρ, A, λ, and D are the resistance at the highest temperature, the resistivity (on the order of 10^{-7}), the cross-sectional area (on the order of 10^{-16}), the effective constant for the MCI (on the order of 10), and the diffusion constant for the MCI, respectively. In the data fitting, D was used as only a free parameter, fixing the R_n at the one end.

The temperature dependence can be classified into the following two voltage regions: (a) *High-voltage region*: the lower four features (0.144–0.124 V of $V^{1/2}$). The temperature dependence can be fitted by Eq. (1) at all temperatures measured. This high-voltage region exists between V_{1D} and V_{CB}. (b) *Low-voltage region*: upper eight features (0.114–0.032 V). This low-voltage region is smaller than V_{CB}. The temperature dependence can be classified into the following two regimes by the T_c, defined as the temperature at which the deviation starts to emerge from the linear fitting by Eq. (1): (i) High-temperature region ($T_c>T$), which can be well fitted by Eq. (1). (ii) Low-temperature region ($T_c<T$), in which the deviations appear from Eq. (1).

In the high-temperature region, it should be noted that the slope value, α, of the linear part increases with a decrease of voltage as shown in Fig. 3. Figure 4(a) shows the inverse of the slope value (α^{-1}) versus $V^{1/2}$ obtained from Fig. 3. The interpretation assuming the linearity shown by the dotted line will be discussed in Sec. III C. In addition, T_c interestingly shifts to the lower-temperature region in this increase of α in Fig. 3. Figure 4(b) shows the T_c-vs-$D^{1/2}$ relation. D was determined from the parameter fitting to α by Eq. (1) at each voltage in Fig. 3. The T_c-vs-$D^{1/2}$ relation is mostly linear. Since it is the manifestation of the correlation of the CB with the MCI in the Ni wire, the interpretation is discussed in Sec. III D.

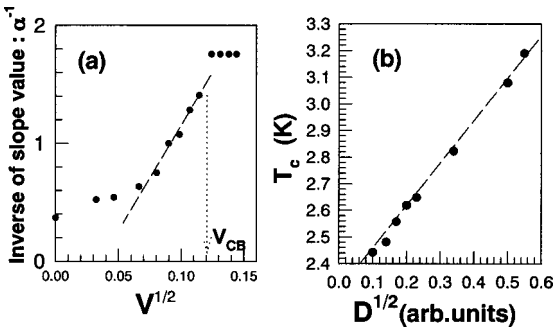

FIG. 4. (a) $V^{1/2}$ dependence of the inverse of the slope value (α) of the linear $\delta R(T)/R_n$-vs-$T^{-1/2}$ parts obtained from Fig. 3. α drastically increases within V_{CB}. The dotted line means a linear relation is assumed. (b) T_c in Fig. 3 vs the square root of the thermal diffusion coefficient ($D^{1/2}$) of the MCI, obtained from α. It implies a mostly linear relation as shown by the dotted line.

Figure 5 shows the dependence of the G_0-versus-temperature relation on the Ni-wire diameter (ϕ). In each feature, the linear G_0-versus-temperature relation and T_c can be clearly observed. They are more obvious than those in the inset of Fig. 2. The inset shows the dependence of T_c on ϕ with the T_c in the inset of Fig. 2. It exhibits a mostly linear T_c-vs-ϕ relation, although the sample number is only 3. It is discussed in Sec. III E that this linear relation is consistent with the linear T_c-vs-$D^{1/2}$ relation.

Figure 6(a) shows the magnetic field (B) dependence of the G_0-versus-temperature relation of the sample with $\phi=32$ nm in Fig. 5. The magnetic field dependence remarkably changes around T_c. G_0 is mostly independent of the magnetic field at temperatures below T_c, whereas positive magnetoconductance emerges at temperatures above T_c. This result strongly supports the actual presence of T_c with different mechanisms at the temperatures above and below T_c. Figure 6(b) shows the magnetic field dependence of the I-V curves in each temperature region. The change of the

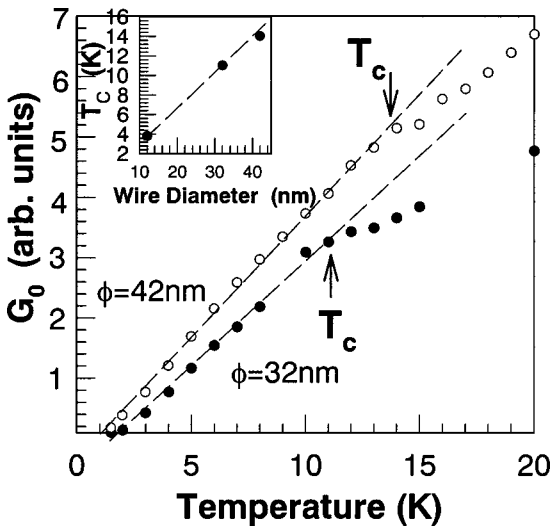

FIG. 5. Dependence of G_0-vs-temperature features on the Ni-wire diameters (ϕ). Only ϕ was varied, while keeping the tunnel junction parameters constant. Inset: Dependence of T_c on ϕ with the T_c of the inset in Fig. 2. It supports the linear T_c-vs-$D^{1/2}$ relation in Fig. 4(b).

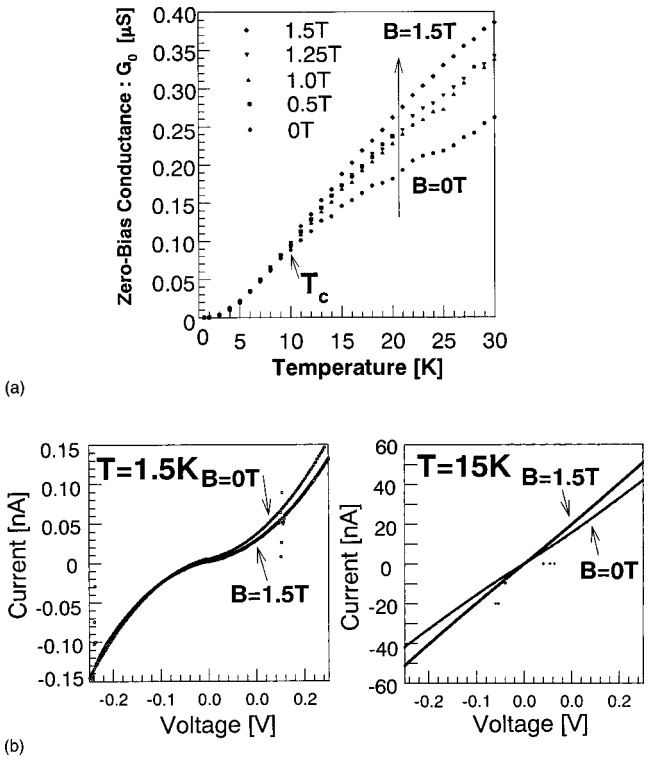

FIG. 6. (a) Magnetic field (B) dependence of G_0 vs temperature in the sample with $\phi = 32$ nm shown in Fig. 5. G_0-vs-temperature relation is mostly independent of B at temperatures below T_c(CB) regime), whereas a positive magnetoconductance appears at temperature above T_c (1D MCI regime). (b) B dependence of I-V curves at the temperatures above and below T_c.

I-V curve is quite asymmetric at $T = 1.5\,\mathrm{K}$ ($< T_c$). The current is reduced in the positive-voltage region, whereas it mostly does not change in the negative-voltage region. The currents lead to mostly G_0 independent of the magnetic field. On the other hand, the change of I-V is symmetric at $T = 15\,\mathrm{K}$ ($> T_c$). Absolute values of the current are greatly increased in the entire voltage regions, leading to the positive magnetocoductance. The possible mechanisms are speculated upon in Sec. III F.

III. INTERPRETATION AND DISCUSSION

A. Coulomb blockade in an array of single junctions located in parallel

The G_0 anomaly with the linear G_0-versus-temperature relation shown in Fig. 2 can be interpreted as a result of CB from the following two viewpoints.

1. Zeller-Giaever report of the CB

Zeller and Giaever[15] experimentally reported on the observation of the G_0 anomaly and its linear G_0-versus-temperature relation. The system was an array of Sn nanoparticles with the surface oxide layers located in parallel (i.e., double nano-tunnel-junction array system). The linear G_0-versus-temperature relation, which was observed at temperatures below about 4 K in the Sn array with a mean radius of 15 nm, is qualitatively similar to our observation, although the quantitative discussion is difficult because G_0 was presented in arbitrary units in Ref. 15. They theoretically explained the G_0 anomaly by the capacitance model (i.e., charging effect) of one Sn nanoparticle. It has basically the same meaning as the orthodox theory of the CB. The linear G_0-versus-temperature relation was also explained by the contribution of many particles, located in parallel, with distributed charging energy (i.e., V_c) as follows:

$$G_0(T) = \int_0^\infty n(V_c)\exp(-eV_c/kT)\,dV_c, \tag{2}$$

where $n(V_c)$ is the area of all particles with activation energy $e^2/2C \pm eV_D = eV_c$. This equation can result in the linear G_0-versus-temperature relation by assuming $n(V_c)$ as a constant and taking it out of the integral. It is, however, not relevant to directly employ Eq. (2) for an explanation of our result, because Eq. (2) does not include consideration of the tunnel probability based on Fermi's golden rule. Only Maxwell-Boltzmann statistics are introduced as the number of particles with V_c in it.

Here, extending this model, we try to simply explain our linear G_0-versus-temperature relation by using the orthodox theory of the CB. The tunneling probability (Γ) for one STJ is simply given by the following equation including Fermi's golden rule, when the tunnel transition probability is assumed to be $(e^2R_t)^{-1}$ and the influence of external environment is neglected:

$$\Gamma(V,T) = (1/e^2R_t)\int_{-\infty}^{\infty} dE\, f(E)[1 - f(E+\delta E)]$$

$$= \frac{V - e/2C_j}{eR_t}\{1 - \exp[-(\delta E/kT)]\}^{-1}, \tag{3}$$

where δE is the resultant energy change of a system by a single electron tunneling (SET) event (i.e., $\delta E = eV - e^2/2C_j$). C_j and R_t are the junction capacitance and the tunnel resistance of the single junction, respectively. Equation (3) can be rewritten by placing $V = 0$ and taking into account the $e^2/2C_j(=E_c) \gg kT$ as follows:

$$\Gamma(0,T) = \frac{1}{2C_jR_t}\exp[-(E_c/kT)]. \tag{4}$$

This equation gives the temperature dependence of zero-bias tunnel probability for one single junction. In this process, a thermally excited electron occasionally causes the SET event. More detailed calculations for the tunnel transition probability lead to the temperature dependence of G_0 in the orthodox theory. Here, the contribution of many single junctions located in parallel with the distributed E_c can be introduced by integrating E_c in Eq. (4) as follows:

$$\Gamma_{\mathrm{tot}}(0,T) = \frac{1}{2C_jR_{t(\mathrm{tot})}}\int_0^\infty \exp[-(E_c/kT)]\,dE_c$$

$$= \frac{k}{2C_jR_{t(\mathrm{tot})}}T, \tag{5}$$

where $R_{t(\mathrm{tot})}$ is the total R_t. Equation (5) actually implies the linear G_0-versus-temperature relation that is qualitatively consistent with our observation.

The coefficient of Eq. (5) also quantitatively agrees with the experimental result (the slope value of the linear part of the inset of Fig. 2) as follows. Since we used a simple tunnel transition probability in Eq. (3), R_t in Eq. (4) should be replaced by the total R_t in Eq. (5). In contrast, C_j should not be replaced by the total C_j, because the coupling among the neighboring junctions is weak in our system owing to the sufficiently large junction spacing ($\sim$30 nm). Here, $R_{t(\mathrm{tot})}$ can be estimated to be on the order of $10^2\,\Omega$ from the R_t of $10^6\,\Omega$ and the number of junctions on the order of 10^4. C_j is also estimated to be on the order of 10^{-17} F from Refs. 10 and 11. Thus coefficient of temperature in Eq. (5) can be estimated to be on the order of 10^{-8}. This value is in good agreement with the slope value of the linear part (order of 10^{-8}/1 K) in the inset of Fig. 2. Therefore, one can conclude that the linear G_0-versus-temperature relation can provide qualitatively and quantitatively strong evidence for the CB in the array of junctions that are located in parallel form.

Although our system is a STJ array biased by voltage, this calculation is relevant, because of the presence of high $\mathrm{Re}[Z_t(\omega)]$ with high R_L and the zero-bias tunneling probability. For more accurate discussion, both the phase correlation function $[P(E)]$ and the actual distribution function of the junction parameters have to be at least introduced into Eq. (3).

2. Cleland-Schmidt-Clarke report

There is one large difference between our observation and the Zeller-Giaever observation. The extrapolation of the linear G_0-versus-temperature (T) relation to $T=0$ K leads to no G_0 in that of Zeller and Giaver, whereas a nonvanishing G_0 exists even at $T=0$ K in our case. From this viewpoint, the Cleland-Schmidt-Clarke report is comparable with our observation, which discusses the G_0 anomaly, which strongly depends on the transmission line resistance R_L, and the normalized zero-bias resistance (R_0/R_t)-vs-1/T relation. The relation exhibited a saturation (flattening) at low temperatures near $T=0$ K and a linearity at high temperatures. Since the R_0/R_t-vs-1/T relation can be basically replaced by the G_0-vs-T relation, both the saturation and the linear R_0/R_t-vs-1/T relation can qualitatively correspond to our observations (i.e., nonvanishing G_0 and linear G_0 vs T, respectively).

Their system was similar to ours, because the single junction was directly connected to the 2-μm-wide Ni transmission line. Since they explained the G_0 anomaly as a CB following a part of the PC theory and successfully turned out environmental effect on the CB (i.e., influence of the high R_L), our results can be also qualitatively called a CB. The saturation at low temperatures was also explained by employing a fluctuation charge q, caused by Nyquist voltage noise in the transmission line and obtained from quantum Langevin equation, in Eq. (4). This is consistent with our result, because there is a possibility of the presence of a Nyquist phase-breaking process also in our Ni nanowire as discussed in Sec. III D later. The only main difference between our observation and the observation of Ref. 3 is that Ref. 3 also indicates that even one single junction can exhibit a linear G_0-vs-T relation based on q.

When it is concluded that the G_0 anomaly in Fig. 2(a) is a CB from the discussion above, our single-junction system at least must satisfy the following four necessary conditions:[10] (1) $R_t \gg R_Q$, (2) $E_c \gg kT$, (3) $\mathrm{Re}[Z_t(\omega)] \gg R_Q$, and the (4) half-width of distributed tunnel junction parameters is less than 25%. The first and second conditions must be satisfied in any tunnel-junction system. The fourth condition, based on Mullen's calculation,[10] is required only for the parallel junction array system. The third condition is of core importance only for STJ systems. It was already confirmed in Refs. 10 and 11 that our STJ system satisfied all of these conditions, except for the following problem with parasitic capacitance (C_{par}). When we defined $L=\tau c$ (where $\tau \sim h/eV$ and c is the velocity of light in vacuum) as the geometry for an effective C_{par} as in the horizontal model, the C_{par} in the L was much larger than that estimated from the observed CB.[10,18] To explain this difference, we may have to select a smaller velocity instead of c in our very disordered Ni nanowire. This problem is not yet clarified even in this work.

Here, the third condition is the key factor for this work. The measurement of the resistance (R_{Ni}) of the single Ni wire by STM revealed that R_{Ni} was near 120 kΩ, which was larger than R_Q. The Ni wire is also directly connected to the single junction. Therefore, one can infer that the Ni wire automatically act as the role of high $\mathrm{Re}[Z_t(\omega)]$ and R_L in our system. The R_{Ni} of 120 kΩ is, however, three orders higher than that in bulk Ni. It is discussed in the next section that the origin for this anomalous high R_{Ni} lies in the mutual Coulomb interaction caused by disorder.

B. Mutual Coulomb interaction in disordered Ni nanowire at high voltages

The linear G-vs-$V^{1/2}$ relation at voltages above $V_{1\mathrm{D}}$ in Fig. 2 quantitatively indicated the presence of a three-dimensional (3D) MCI, in the disordered Ni-nanowire, following the Altshuler-Aronov formula.[10,14] In contrast, the temperature dependence in the first high-voltage region ($V_{\mathrm{CB}} < V < V_{1\mathrm{D}}$) of Fig. 3 was successfully fitted by Eq. (1) in the entire temperature region. It qualitatively implies the presence of a 1D MCI following the Altshuler-Aronov theory. One can confirm its relevance by comparing the thermal diffusion length l_T with the localization length ξ_{loc}. They can be estimated as follows, by using D, which gives the best fit to the linear slope of the high voltages of Fig. 3, and the R_{Ni} of 120 kΩ for conductivity σ, respectively:

$$l_T = (\hbar D/kT)^{1/2} \sim 10^{-8}, \tag{6}$$

$$\xi_{\mathrm{loc}} = (2\hbar/e^2) A\sigma \sim 10^{-7}. \tag{7}$$

Since ξ_{loc} is actually one order larger than l_T and wire length, it is reconfirmed that the Ni wire is in the weak localization regime.

In addition, since this l_T is larger than ϕ and smaller than wire length, it quantitatively supports the presence of one dimension of the MCI. Thus, it is concluded that the 1D MCI is the dominant conductance mechanism in the high-voltage region and that $V_{1\mathrm{D}}$ is the transition voltage from the 3D to the 1D MCI regimes with decreasing voltage. Since l_T becomes larger than ϕ at $V_{1\mathrm{D}}$ with decreasing voltage in this transition, the MCI loses two dimensions at $V_{1\mathrm{D}}$ at the same time, because the cross section of Ni wire has two dimensions. It results in the direct transition from the 3D to 1D MCI regimes, which is consistent with our observation of the absence of the 2D MCI regime. Since this 1D MCI can lead to an impedance higher than that of the 3D MCI because of

the stronger scattering rate, it can play the role of the high $\mathrm{Re}[Z_t(\omega)]$ and R_L for the CB. However, note that any CB-related characteristics are not observed in the voltage region higher than V_{CB} in spite of this high-impedance EME. The reason is discussed in Sec. III D.

Why l_T increases with decreasing voltage can be qualitatively interpreted as follows. In the formula of l_T, only the diffusion constant D has a voltage dependence because of the following equation:

$$D = v_F^2 \tau_{e\text{-}e}/d, \tag{8}$$

where v_F, $\tau_{e\text{-}e}$, and d are the Fermi velocity, the relaxation (collision) time for electron-electron scattering, and the sample dimension, respectively.[14] Although v_F^2 decreases with decreasing voltage, $\tau_{e\text{-}e}$ can increase with decreasing the electron-electron scattering rate (i.e., $1/\tau_{e\text{-}e}$). If the increase of $\tau_{e\text{-}e}$ quantitatively exceeds the decrease of v_F^2, D can increase with decreasing voltage.

C. CB and 1D MCI temperature regimes distinguished at T_c at low voltages

In the low-voltage region, T_c separates the temperature dependence into two regions. At low temperatures ($T < T_c$), conductance (G)-versus-temperature features show a mostly linear relation. In particular, it can be well represented by the linear G_0-versus-temperature regime (below 4 K) shown in the inset of Fig. 2. This is a straightforward indication that the temperature region below T_c is the CB temperature regime. This CB temperature regime emerges only at voltages below V_{CB} at $T = 1.5\,\mathrm{K}$. In this sense, V_{CB} can be the transition voltage from the 1D MCI to the CB voltage regimes. In contrast, the linearity at high temperatures ($T > T_c$) indicates the possible presence of the Altshuler-Aronov 1D MCI as well as that of the high-voltage region mentioned in the preceding section.

There is, however, one large difference in that the slope value α of the linear part drastically increases with reducing voltage, as shown in Fig. 4(a). If one possibly assumes that this relation is mostly linear except for the saturation around 0 V as shown by the dotted line in Fig. 4(a), the increase of α can be also qualitatively interpreted by the Altshuler-Aronov formula for the voltage dependence of $\tau_{e\text{-}e}$ (i.e., linear $\tau_{e\text{-}e}^{-1/2}$ vs $V^{1/2}$) in the 1D MCI as follows.[14] From Eq. (1) and the discussion in the preceding section, α can have the following relation with $D^{1/2}$ and $\tau_{e\text{-}e}$:

$$\alpha \propto D^{1/2} \propto \tau_{e\text{-}e}^{1/2}. \tag{9}$$

Thus, if the linear α^{-1} vs $V^{1/2}$ relation is assumed, one can attain the following relation:

$$\alpha^{-1} \propto \tau_{e\text{-}e}^{-1/2} \propto V^{1/2}. \tag{10}$$

This qualitatively agrees with the linear $\tau_{e\text{-}e}^{-1/2}$-vs-$V^{1/2}$ relation proposed by Altshuler and Aronov mentioned above. This relation implies that the scattering rate of MCI (i.e., $\tau_{e\text{-}e}^{-1}$) decreases with a decrease of the applied voltage in 1D disorder systems. The reason for the saturation around 0 V, however, is not revealed here. It indicates that $\tau_{e\text{-}e}^{-1}$ does not become zero even at $V = 0$. There may exist other interesting mechanisms (e.g., the influence of thermal diffusion at finite temperature). In this case, linearity cannot be assumed and hence novel explanations for this increase of α will have to be introduced. We conclude that the high-temperature regime ($T > T_c$) is also the 1D MCI regime as well as that in the first voltage region ($V > V_{\mathrm{CB}}$), based on only the presence of the linear $\delta R/R_n$-vs-$T^{-1/2}$ relation and the assumption of linearity in Fig. 4(a).

Consequently, one can conclude that T_c is the phase-transition temperature from the 1D MCI to the CB temperature regimes with decreasing temperature. This means that the G_0 anomalies, which are observed at temperatures above 7 K ($> T_c$) in Fig. 2, are simply due to the MCI following the Altshuler-Aronov theory. In contrast, anomalies at $T = 1.5\,\mathrm{K}$ ($< T_c$) originate from the CB. This is consistent with V_{CB} being distinct only at $T = 1.5\,\mathrm{K}$ in the G-vs-$V^{1/2}$ curves in Fig. 2, because even the largest T_c is 3.2 K as shown in Fig. 4(b). However, note that the 1D MCI in the Ni wire never disappears even in this CB temperature regime ($T < T_c$). It plays the key role in yielding the CB as the high $\mathrm{Re}[Z_t(\omega)]$ and R_L in the CB temperature regime. As mentioned in the next section, this is supported by the fact that this CB temperature regime is very sensitive to the diffusion constant (D) of the MCI. Here, MCI is basically an elastic process. Since, however, the origin of this MCI is the electron-phonon scattering by a disordered potential, the tunneling electron may at least transfer the E_c to there, although it is a small energy transfer.

D. Correlation of CB with 1D MCI in Ni wire

For the correlation between the CB and 1D MCI in the Ni wire, we can find the most important and interesting feature in this work. T_c shifts to the lower-temperature region with increasing α (i.e., D) through decreasing voltage as shown in Fig. 3. The T_c-vs-$D^{1/2}$ curve exhibits a mostly linear relation as shown in Fig. 4(b). Since D is assumed to be proportional to $\tau_{e\text{-}e}$ as shown in Eq. (9), this linearity indicates that T_c strongly depends on $\tau_{e\text{-}e}$ in the Ni wire. Although there may be some differing interpretations for this linear T_c-vs-$D^{1/2}$ relation, we propose one possible explanation as follows. Any MCI process yields some kind of fluctuations. In particular, Altshuler, Aronov, and Khmelnitsky pointed out that multiple quasielastic MCI processes dominate the phase-breaking process in 1D and 2D disordered conductors in the absence of other phase-breaking mechanisms, the so-called Nyquist phase breaking.[17] According to Ref. 17, an energy quantum (E_N) of fluctuating field can be given by

$$E_N = \hbar\omega_N \sim \hbar[T/D^{1/2}N(E)]^{2/3}, \tag{11}$$

where $\hbar$, ω_N, and $N(E)$ are the Dirac constant, the frequency of the fluctuating field, and the density of states in a 1D conductor, respectively. Since V_{CB} is in the 1D MCI voltage regime, Eq. (11) can be applied for this discussion. If the charging energy (E_c) of the CB is smaller than E_N, the CB will be smeared out by the fluctuation even if the temperature satisfies the thermal condition (i.e., $E_C \gg kT$). Hence, when E_N is equal to E_C, Eq. (12) is given by Eq. (11):

$$T_c \sim [(E_c/\hbar)^{3/2} N(E)^{-1}] D^{1/2}. \tag{12}$$

When it is assumed that both E_c and $N(E)$ are basically constants, this equation immediately indicates the linear T_c-vs-$D^{1/2}$ relation. Here, E_C is actually a constant for the same sample. In contrast, since $N(E)$ in a 1D conductor is generally proportional to inverse of E and applied voltage, it is not constant. $N(E)$ here, however, can be almost a constant, because this voltage region (i.e., $V<V_{\mathrm{CB}}$) is around 0 V. In Fig. 4(b), the extrapolation to $D^{1/2}=0$ leads to $T_c=2.3\,\mathrm{K}$. This may mean that the CB temperature regime survives up to 2.3 K, even if the Ni nanowire is in the strong-localization regime.

This explanation implies that E_C and the E_N compete at T_c, which is characterized by a diffusion constant D depending on the $\tau_{e\text{-}e}^{-1}$ as shown in Eqs. (9) and (12). As applied voltage is decreased, D becomes larger, because of the decrease of $\tau_{e\text{-}e}^{-1}$. It can reduce E_N in Eq. (11). As a result, since E_C exceeds E_N, T_c increases in Eq. (12). In the other words, the CB temperature regime can be smeared out by the fluctuation energy quantum E_N of the Nyquist phase-breaking process in the EME. Of course, since the CB requires essentially no phase coherence, the phase-breaking process itself does not directly affect the CB except for the case of spin coherence. This result, however, directly indicates that the field fluctuation caused by phase breaking in the EME can affect the CB in single-junction systems. Here, as discussed in Sec. III A, our observation qualitatively agreed with the Cleland-Schmidt-Clarke observation,[3,10,18] which was explained by introducing the fluctuation charge q caused by a Nyquist voltage noise in the external transmission line.[3] This is consistent with the presence of the Nyquist phase-breaking process in the Ni nanowire in our system.

This discussion is also consistent with PC theory.[2] One can simply replace the excitation energy of an environmental mode ($\hbar\omega_S$) in PC theory to the fluctuation energy quantum $\hbar\omega_N$ and compare with E_C. In this sense, the tunneling electron can transfer its E_C by exciting $\hbar\omega_N$ in our system. Here, this MCI in the Ni wire also plays the role of high R_L to avoid the external environmental fluctuation in our system, leading to the CB. However, when too large an E_N caused by the high $\tau_{e\text{-}e}^{-1}$ exists in our Ni wire, it can excite too large $\hbar\omega_N(\hbar\omega_S)$. In such a case, the Ni wire can no longer act as high R_L, because the Ni wire becomes only a large Nyquist noise source. This is also consistent with PC theory, because if E_C is much smaller than the excited energy of environmental mode $\hbar\omega_S$, the phase correlation function $[J(t)]$ and phase fluctuation $\tilde{\varphi}$ of the external environment approach to zero and hence the charge fluctuation $\tilde{Q}$ on the junction surface diverges through the commutation relation $[\tilde{\varphi},\tilde{Q}]=ie$ in PC theory. It easily smears out the CB voltage. Here, since the high $\tau_{e\text{-}e}^{-1}$ (i.e., a decrease of α) is caused by the increase of voltage in Figs. 2 and 3, it is suggested that the smearing out of the CB temperature regime in the $V>V_{\mathrm{CB}}$ is due to this extremely large $\tau_{e\text{-}e}^{-1}$ at 1.5 K in Fig. 2. This explanation implies the necessity of the optimized $\tau_{e\text{-}e}^{-1}$ when the MCI is the origin of the high R_L for the CB in the single-junction system.

E. Wire-diameter dependence of T_c

In order to reconfirm this discussion, a quantitative comparison of the slope of the value shown in Fig. 4(b) with the coefficient of Eq. (12) is required. However, since the coefficient has not been exactly determined in any past works, it will be difficult at this stage. In the preceding section, a decrease of the applied voltage varied the diffusion constant D. In contrast, since D also strongly depends on ϕ, it is expected that different ϕ also shift T_c. The result exhibits mostly linear V_c-vs-ϕ relation as shown in the inset of Fig. 5. Here, D has the following relation with the electron density n and the cross-sectional area of Ni wire A:

$$D\propto 1/n\propto A=\pi(\phi/2)^2. \tag{13}$$

Thus, T_c can have the following relation with D, when the linear T_c-vs-ϕ relation actually exists:

$$T_c\propto\phi=2(A/\pi)^{1/2}\propto D^{1/2}. \tag{14}$$

Therefore, the linear T_c-vs-ϕ relation in Fig. 5 qualitatively supports the presence of the linear T_c-vs-$D^{1/2}$ relation. In Fig. 5, the extrapolation to $T_c=2$ K results in ϕ of about 5 nm. It may mean that around ϕ, the Ni nanowire may enter a strong-localization regime as discussed above.

The G_0-vs-T relations in Fig. 5 have the following two slight differences from that in the inset of Fig. 2(a): (1) G_0 saturates around $T=1.5\,\mathrm{K}$ with a value of about 10^{-8} S. (2) The data fittings by Eq. (1) at temperature above T_c become rougher, although they are still fitted with different slopes. Although these may originate from large wire diameters, the origins are not clear.

F. Magnetic field dependence of the G_0-vs-temperature relation and I-V curves

The magnetic field (B) dependence of the G_0-vs-temperature (T) relation is drastically varied around T_c as shown in Fig. 6(a). This result obviously supports the presence of a T_c with a physical meaning, although T_c was not distinct in the inset of Fig. 2(a) and Fig. 3. It also implies the presence of quite different G_0 mechanisms between the temperature regions below and above T_c. In fact, the symmetry of the I-V curves on the applied B was quite different between the two temperature regions, as shown in Fig. 6(b).

Here, applying a positive voltage corresponds to the injection of an electron from the Al substrate side, whereas a negative voltage corresponds to the injection from the Ni-wire side. The origin of Fig. 6(b) may be speculated based on the following, although it is not the aim of this work.

The change of the I-V curve by the applied B is quite asymmetric in the CB temperature regime [$T=1.5\,\mathrm{K}$ ($<T_c$)]. The most asymmetric part in our structure is the single tunnel barrier layer that exists between one end of the Ni nanowire and the Al substrate. When the CB is the dominant mechanism for electron transport in the system, the change in the I-V curve with B will easily reflect this asymmetry from the following speculation. There may exist three effects related to the applied B in the $\mathrm{Al/Al_2O_3/Ni}$ wire (i.e., in Al and Ni) system: (a) differences in spin-flip scattering, (b) different Zeeman energies (spin magnetic moments), and (c) differences in the spin-orbit interaction. In the first case, the electrons in the d orbit of the Ni nanowire are strongly

spin-polarized by the applied B, whereas there is no spin polarization in the Al substrate. Thus, only when the electrons tunnel through from the Al to the Ni wire is a large spin-flip scattering caused at the entrance of the Ni wire. Consequently, the CB is enhanced in this process, because an electron needs more energy to overcome the spin-flip scattering in addition to the E_C. In contrast, when the electrons tunnel into the Al, there is basically no influence of the spin polarization. Thus, the I-V curve is mostly independent of B. These may lead to the asymmetric I-V curves with the applied B.

Also, in the second case, when electrons tunnel into the Ni wire, additional energy for electrons is required in addition to E_C, because of the Zeeman energy in the Ni. In contrast, this means that electrons can tunnel into the Al with smaller energies because of the Zeeman energy of Ni. Therefore I-V curves should strongly depend on B in all the voltage regions in this process. Hence, this case does not seem to explain the B-independent feature in the negative-voltage region in Fig. 6(b). The third case may be less possible because Ni has a very small spin-orbit interaction.

On the other hand, the change of the I-V curve with applied B is quite symmetric in the 1D MCI regime [$T=15$ K ($>T_c$)]. When the CB has vanished in this high-temperature region, the tunnel barrier becomes a simple tunneling resistance without E_C. Thus, the electron transport is dominated by the Ni nanowire, which has a symmetric structure. It is consistent with the symmetric I-V change with the applied B. As a typical example, positive magnetoconductances (MC) have been-observed in weak localization as a result of the phase-interference effect of electron waves [e.g., $G \propto \log(B)$ in 2D weak localization]. Our case, however, may not correspond to it, because the Altshuler-Aronov formula for the MCI, which exists in our Ni wire, took into account only charge of electrons for quantum correction. In addition, the B dependence of the 1D MCI is not clearly reported, especially in ferromagnetic nanowires. Thus it is difficult to identify the origin of positive MC and also its correlation with T_c from this B dependence. In order to reveal the mechanisms for magnetoconductance, detailed measurements and analyses are indispensable taking into account the physics ferromagnetic nanowire.

III. CONCLUSION

The CB which depends on the 1D MCI in the EME was reported in a disordered Ni nanowire/Al_2O_3/Al array in parallel structure, fabricated using nanoporous alumina film. The observed G_0 anomaly and its linear G_0-versus-temperature relation qualitatively agreed with the Zeller-Gíaever and Cleland-Schmidt-Clarke reports of the CB. It was also quantitatively verified from the extended model in Ref. 15 of the tunnel-junction array. At $V>V_{CB}$, only the 1D MCI following the Altshuler-Aronov formula in the disordered Ni wire governs the conductance mechanism. In contrast, at $V<V_{CB}$, the CB emerged accompanied with 1D MCI, also following the Altshuler-Aronov formula. The 1D MCI in the Ni wire played the key roles of high Re[$Z_t(\omega)$] and R_L in phase-correlation theory for our CB in the single-junction system. It was supported by the fact that the CB was very sensitive to the diffusion constant D of the MCI, yielding the linear T_c-vs-$D^{1/2}$ relation. This relation was interpreted as a result of the correlation between the charging energy E_C of the CB and the energy quantum E_N of the fluctuating field in the Ni wire. Tunneling electrons could transfer E_C to the EME by exciting this energy quantum E_N ($=\hbar\omega_N$), although it is a small energy transfer, consistent with PC theory. In contrast, MCI also acted as high R_L. Too large a mutual Coulomb scattering rate, however, yielded large E_N, smearing the CB by the commutation relation $[\tilde{\varphi},\tilde{Q}]=ie$. This linear T_c-vs-$D^{1/2}$ relation was reconfirmed by the linear wire-diameter dependence of T_c. The presence of T_c and different conductance mechanisms classified at T_c were also obviously reconfirmed by the magnetic field dependence of the G_0-versus-temperature relation.

This work reported on the correlation of the CB with the 1D MCI in the external environment in a single-junction system. In contrast, when phase coherence of electron waves is conserved in disordered materials, a variety of mesoscopic phenomena emerges (e.g., AB effect, UCF, weak localization). These phenomena will bring us novel mesoscopic phenomena associated with single-electron tunneling. We plan to report on it by utilizing our porous alumina film (e.g., by depositing multiwalled carbon nanotube into the nanopores).[19]

ACKNOWLEDGMENTS

We are grateful to D. Averin, B. L. Altshuler, C. Marcus, X. Wang, M. Ueda, Y. Yamamoto, J. M. Xu, A. J. Bennett, and W. D. Oliver for fruitful discussion and suggestions, and the Foundation for the Promotion of MST Japan for clear TEM images. This work was partially supported by the MST, and the scientific research project both on the basic study B and on the priority area of Japanese Ministry of Education, Science, Sport, and Culture. J. H. also sincerely thanks Yuki, Wakana, and Rika for continuous encouragement.

[1] D. V. Averin and K. K. Likharev, in *Mesoscopic Phenomena in Solids*, edited by B. L. Altshuler, P. A. Lee, and R. A. Webb (North-Holland, 173, 1991); in *Single Charge Tunneling*, edited by H. Grabert and M. H. Devoret (Plenum, New York, 1991).

[2] G.-L. Ingold and Yu. V. Nazarov, *Single Charge Tunneling*, Ref. 1, p. 21.

[3] A. N. Cleland, J. M. Schmidt, and J. Clarke, Phys. Rev. Lett. **64**, 1565 (1990).

[4] A. Yacoby, M. Heiblum, D. Mahalu, and H. Shtrikman, Phys. Rev. Lett. **74**, 4047 (1995).

[5] H. Akera *Abstract of Int. Nat. Sym. Nano-Physics and Electronics (NPE) 97(TOKYO), 83 (1997).*

[6] S. Tarucha, D. G. Austing, T. Honda, R. J. van der Hage, and L. P. Kouwenhoven, Phys. Rev. Lett. **77**, 3613 (1996).

[7] S. Drewes and S. R. Renn, Phys. Rev. Lett. **80**, 1046 (1998).

[8] Ya. M. Blanter, A. D. Mirlin, and B. A. Muzykantskii, Phys. Rev. Lett. **78**, 2449 (1997).

[9] J. A. Folk, S. R. Patel, S. F. Godijn, A. G. Huibers, S. M. Cronenwett, and C. M. Marcus, Phys. Rev. Lett. **76**, 1699 (1996).
[10] J. Haruyama, D. Davydov, D. Routkevitch, D. Ellis, B. W. Statt, M. Moskovits, and J. M. Xu, Solid-State Electron. as the proc. NPE'97, 42, 1257 (1998).
[11] D. Davydov, J. Haruyama, D. Routkevitch, D. Ellis, B. W. Statt, M. Moskovits, and J. M. Xu, Phys. Rev. B **57**, 13 550 (1998).
[12] D. Routkevitch, A. A. Tager, J. Haruyama, D. Almawlawi, M. Moskovits, and J. M. Xu, IEEE Electron Device Lett. **43**, 1646 (1996); A. Tager, D. Routkevitch, J. Haruyama, D. Almawlawi, M. Moskovits, and J. M. Xu, in *Future Trends in Microelectronics*, edited by S. Luryi, J. M. Xu, and A. Zalavsky, NATO Advanced Studies Institute, Series E, 171 (1996).
[13] Yu. V. Nazarov, [Sov. Phys. JETP **68**, 561 (1989)]; in *Single Charge Tunneling*, Ref. 1, p. 99.
[14] B. L. Altshuler and A. G. Aronov, in *Electron-Electron Interactions in Disordered Systems*, edited by A. L. Efros and M. Pollak (North-Holland, 1985); B. L. Altshuler and A. G. Aronov, Solid State Commun. **30**, 115 (1979).
[15] H. R. Zeller and I. Giaever, Phys. Rev. **181**, 789 (1969).
[16] S. Kobayashi, Surf. Sci. Rep. **16**, 1 (1992).
[17] B. L. Altshuler, A. G. Aronov, and D. E. Khmelnitsky, J. Phys. C **15**, 7367 (1982).
[18] Yu. V. Nazarov, [Sov. Phys. JETP **68**, 561 (1989)]; J. P. Kauppinen and J. P. Pekola, Phys. Rev. Lett. **77**, 3889 (1996); P. Delsing, K. K. Likharev, L. S. Kuzmin, and T. Claeson, Phys. Rev. Lett. **63**, 1180 (1989).
[19] J. Haruyam, I. Takesue, and Y. Sato, Appl. Phys. Lett. (to be published); J. Haruyam, I. Takesue, Y. Sato, K. Hijioka, in Quantum Mesoscopic Phenomena and Mesoscopic Devices in Microelectronics, edited by I. Kulik, NATO ASI book series (2000).